Analysis of alternative flat representations of a UAV for trajectory generation and tracking

Huu-Thinh Do, Ionela Prodan, Florin Stoican

Analysis of alternative flat representations of a UAV for trajectory generation and tracking

Huu-Thinh DO
Univ. Grenoble Alpes, Grenoble INP
LCIS, F-26000, Valence, France
huu-thinh.do@lcis.grenoble-inp.fr

Ionela PRODAN
Univ. Grenoble Alpes, Grenoble INP
LCIS, F-26000, Valence, France
ionela.prodan@lcis.grenoble-inp.fr

Florin STOICAN
Politehnica University of Bucharest
ACSE, Bucharest, Romania
florin.stoican@upb.ro

***Abstract*—Motion planning problems benefit greatly from the properties of differential flatness, which are widely employed for trajectory generation and controller design. This paper aims to highlight the fact that various flat representations of a system can have different implications in the trajectory generation and tracking objectives. In particular, we consider a fixed-wing UAV (Unmanned Aerial Vehicle) and analyze various flat representations. We reformulate the trajectory generation and tracking problem in terms of different flat outputs and analyze the optimal cost, constraints satisfaction, tracking error and computational complexity. Insights on the future work complete the analysis. The research shows promising directions, especially in the area of disturbance rejection and robust control.**

***Index Terms*—Differential flatness, B-spline, Fixed-wing UAV (Unmanned Aerial Vehicle), Trajectory generation and tracking.**

I. Introduction

Flatness theory [1] has proven useful in several stages of designing a control architecture for motion planning problems, i.e., in computing a reference trajectory [2], [3], [4] or in providing a feedback linearizable controller [5], [6]. Having a flat representation of a dynamical system is equivalent with carrying a model inversion (the nonlinear input is mapped in terms of the flat output and linearizes the nonlinear dynamics), which in turn, provides the foundation for both the planning and controlling stages. While there are many formal results for flat output representations [7], [8], to our knowledge, there is no generic algorithm capable to obtain a flat representation for arbitrary dynamics which admit one. An attempt in this direction is provided in [9], however the results is not generic. Furthermore, even when a flat representation is obtained, it may quickly become difficult to handle. Usually the inputs have convoluted expressions in terms of the system's flat output, leading to difficulties when handling constraints and cost formulations.

In [2] and [6] a flat representation and subsequent B-spline parameterization [10] are exploited to construct an optimization problem which, simultaneously, minimizes trajectory length and satisfies various constraints.

However, none of the works aforementioned have addressed the problem of changing the flat output and analyzing the implications of this change for trajectory generation and tracking. Hence, our main contribution is the analysis of alternative flat representations within the same framework of planning and controlling a fixed-wing UAV (Unmanned Aerial Vehicle) and to point out the differences in the performance of the control scheme. More specifically, we reformulate the trajectory generation and tracking problem in terms of different flat outputs and analyze the optimal cost, the constraint satisfaction, tracking error and computational complexity. Note that when the flat output is changed, the construction of constraints and cost function in the trajectory generation process is also altered. Similarly, the feedback linearization control law derived from the model inversion induced by the flat representation will also transform remarkably.

Through this work we want to bring to the community's attention that choosing a certain flat output cascades throughout the rest of the control design procedure (for better or worse). Not in the least, we believe that the research carried here shows promising directions, especially in the area of disturbance rejection and robust control.

The paper is organized as follows. In Section II, we present the main issue of the trajectory generation and the subsequent tracking controller design. This problem will then be implemented with different flat outputs and then discussed in Section III. Section IV provides the numerical simulations. Finally, the conclusions are drawn in Section V.

II. Problem formulation

We first briefly introduce the 2D UAV model used hereinafter and recall the standard problem formulation of trajectory generation and of control design.

A. Fixed-wing UAV model

The UAV kinematic model can be described by the differential equations [2]:

$$\begin{aligned} \dot{x} &= V_a \cos\psi + W_x, \\ \dot{y} &= V_a \sin\psi + W_y, \\ \dot{\psi} &= \frac{g \tan\phi}{V_a}, \end{aligned} \tag{1}$$

where (x, y) and ψ are the position and the heading (yaw) angle. W_x and W_y are the wind velocity components on the x and y axis. Finally, the input signal are the airspeed velocity V_a and the bank (roll) angle ϕ, respectively.

The equations (1) are rewritten in a more compact form as:

$$\dot{\xi} = f(\xi, u), \tag{2}$$

where $\xi = [x\ y\ \psi]^\top \in \mathbb{R}^3$, $u = [V_a\ \phi]^\top \in \mathbb{R}^2$ and $f(\cdot,\cdot) : \mathbb{R}^3 \times \mathbb{R}^2 \to \mathbb{R}^3$ is the state vector field.

Indeed, the nonlinear system (2) is differentially flat when we consider the fact that there exists a flat output vector, $z = \Phi(\xi, u, \dot{u}, \ddot{u}, ...) \in \mathbb{R}^2$, such that the states and inputs can be algebraically expressed in terms of z and a finite number of its derivatives [1].

B. Trajectory generation problem

Further, we recall the B-spline framework used in [2] where the flat output is parameterized in a time interval $[t_0,\ t_N]$ by a set of basis functions $\mathbf{B}_d(t) = [B_{0,d}(t), ..., B_{n,d}]^\top$ through the control points $\mathbf{P} \in \mathbb{R}^{2\times n} = [P_0, ..., P_n]$ such that:

$$z(t) = \mathbf{P}\mathbf{B}_d(t),\ \forall t \in [t_0,\ t_N], \tag{3}$$

where $z(t) \in \mathbb{R}^2$ is the parameterized flat output, n is the number of control points and $(d-1)$ the polynomial order of the B-spline functions, respectively.

Assuming the parameterization in (3) we can now formulate the trajectory generation problem in terms of splines and their associated control points. First, we consider a collection o way-points and their associated time stamps:

$$\mathbb{W} = \{w_k\} \text{ and } \mathbb{T}_\mathbb{W} = \{t_k\}, \tag{4}$$

through which the trajectory has to pass, i.e.,

$$z(t_k) = \omega_k \implies \mathbf{P}\mathbf{B}_d(t_k) = \omega_k. \tag{5}$$

The final objective of this process is to generate profiles, equivalently stated, to find the control points which meet the constraints (5) and minimize the cost function as in [10]:

$$\mathbf{P} = \arg\min_{\mathbf{P}} \int_{t_0}^{t_N} \tilde{\Xi}_i(\mathbf{B}_d(t), \mathbf{P})dt, \tag{6}$$

where $\tilde{\Xi}_i(\mathbf{B}_d(t), \mathbf{P})$ is the energy function at the time instant t defined with the control points as decision variable, known basis function $\mathbf{B}_d(t)$ and the flat output i which will be introduced in Section III.

C. Feedback linearization control design

As proposed in [3], many flat systems can be linearized in closed-loop. In here, using the flat representation we arrive at a controller which, for the nominal dynamics, cancels out the nonlinearities of the dynamics and arrives at a desired linear dynamic [11] in closed-loop.

More specifically, the investigated system is in companion [11] form represented as:

$$\dot{\xi} = f(\xi, u) \tag{7}$$

and an input transformation must be found:

$$\begin{cases} z &= z(\xi, \dot{\xi}, ...), \\ u &= u(v, \xi, \dot{\xi}, ...), \end{cases} \tag{8}$$

so that the nonlinear system dynamics is converted to an equivalent linear time-invariant dynamics:

$$\begin{cases} z^{(n)} &= v, \\ v &= z_{ref}^{(n)} + K_{n-1}e^{(n-1)} + ... + K_0 e, \end{cases} \tag{9}$$

where v is the virtual control input induced from the flat representation, $e = z_{ref} - z$ is the difference between the reference z_{ref} and the feedback value z, and the coefficients K_i with $i \in \{0, 1, ..., n-1\}$ will be chosen such that the poles of the characteristic equation will ensure the stability of the model in closed-loop. Therefore, equation (9) becomes:

$$e^{(n)} + K_{n-1}e^{(n-1)} + ... + K_0 e = 0. \tag{10}$$

III. Analysis of alternative flat outputs

As stated earlier, most results from the literature skip relatively quickly over the choice of a flat output and proceed to the control design steps. In here, we plan to investigate several flat representations and observe how they affect (for better or worse) the procedures of trajectory generation and feedback control design. In Subsection III-A we introduce the four available flat outputs together with the flat representations associated with them. In Subsections B and C, the problem formulation for the trajectory generation and the control design is given when considering the variation in the flat outputs.

A. Various flat representations

In this section we propose different flat representations computed from the chosen flat outputs with no wind perturbation ($W_x = W_y = 0$) and with perfect state measurement.

1) Flat output 1: Consider the following flat output in terms of the system's position:

$$z = \begin{bmatrix} z_1 \\ z_2 \end{bmatrix} = \begin{bmatrix} x \\ y \end{bmatrix}. \tag{11}$$

Next, the remaining states and inputs are expressed as in the equation (12) which is detailed in Table I:

$$\begin{bmatrix} \xi \\ u \end{bmatrix} = \Phi_1\left(z, \dot{z}, \ddot{z}\right). \tag{12}$$

2) Flat output 2: The same process is applied for the second flat representation. In this selection, cylindrical coordinate is used to describe the system:

$$z = \begin{bmatrix} z_1 \\ z_2 \end{bmatrix} = \begin{bmatrix} \sqrt{x^2 + y^2} \\ \arctan\dfrac{y}{x} \end{bmatrix}. \tag{13}$$

The states and inputs then are expressed as in the equation (14) which is detailed in the third column of Table I:

$$\begin{bmatrix} \xi \\ u \end{bmatrix} = \Phi_2\left(z, \dot{z}, \ddot{z}\right). \tag{14}$$

where

$$f_1(z, \dot{z}, \ddot{z}) = \frac{\ddot{z}_2\dot{z}_1 z_1 - \ddot{z}_1\dot{z}_2 z_1}{g\sqrt{\dot{z}_1^2 + z_1^2\dot{z}_2^2}},$$
$$f_2(z, \dot{z}) = \frac{2\dot{z}_1^2\dot{z}_2 + \dot{z}_2^3 z_1^2}{g\sqrt{\dot{z}_1^2 + z_1^2\dot{z}_2^2}}.$$

3) Flat output 3: In here, we take into account the fact that when $[z_1\ z_2]^\top$ is a flat output, $[z_1\ z_2 + \dot{z}_1]^\top$ is also a flat output. Hence, we have that:

$$z = \begin{bmatrix} z_1 \\ z_2 \end{bmatrix} = \begin{bmatrix} x \\ y + \dot{x} \end{bmatrix}. \tag{15}$$

The remaining states and inputs are expressed as in equation (16) which is detailed in the forth column of Table I:

$$\begin{bmatrix} \xi \\ u \end{bmatrix} = \Phi_3\left(z, \dot{z}, \ddot{z}, \dddot{z}\right). \tag{16}$$

TABLE I
FLAT REPRESENTATIONS CORRESPONDING TO DIFFERENT FLAT OUTPUTS.

States and inputs with flat representation	rep. 1 $\Phi_1(\cdot)$	rep. 2 $\Phi_2(\cdot)$	rep. 3 $\Phi_3(\cdot)$	rep. 4 $\Phi_4(\cdot)$
x	z_1	$z_1 \cos z_2$	z_1	$z_2 - \dot{z}_1$
y	z_2	$z_1 \sin z_2$	$z_2 - \dot{z}_1$	$z_1 + \ddot{z}_1 - \dot{z}_2$
$\tan\psi$	$\frac{\dot{z}_2}{\dot{z}_1}$	$\frac{\dot{z}_1 \sin z_2 + \dot{z}_2 z_1 \cos z_2}{\dot{z}_1 \cos z_2 - \dot{z}_2 z_1 \sin z_2}$	$\frac{\dot{z}_2 - \ddot{z}_1}{\dot{z}_1}$	$\frac{\dddot{z}_1 + \dot{z}_1 - \ddot{z}_2}{\dot{z}_2 - \ddot{z}_1}$
V_a	$\sqrt{\dot{z}_1^2 + \dot{z}_2^2}$	$\sqrt{\dot{z}_1^2 + z_1^2 \dot{z}_2^2}$	$\sqrt{\dot{z}_1^2 + (\dot{z}_2 - \ddot{z}_1)^2}$	$\sqrt{(\dddot{z}_1 + \dot{z}_1 - \ddot{z}_2)^2 + (\dot{z}_2 - \ddot{z}_1)^2}$
$\tan\phi$	$\frac{1}{g}\frac{\ddot{z}_2\dot{z}_1 - \ddot{z}_1\dot{z}_2}{\sqrt{\dot{z}_1^2 + \dot{z}_2^2}}$	$f_1(z,\dot{z},\ddot{z}) + f_2(z,\dot{z})$	$\frac{(\dot{z}_2 - \ddot{z}_1)\dddot{z}_1 - (\ddot{z}_2 - \dddot{z}_1)\dot{z}_1}{g\sqrt{\dot{z}_1^2 + \dot{z}_2^2}}$	$g_1(z,\dot{z},\ddot{z},\dddot{z},z^{(4)}) + g_2(z,\dot{z},\ddot{z},\dddot{z})$

4) Flat output 4: The following flat representation is a mix among the system's position, velocity and the acceleration:

$$z = \begin{bmatrix} z_1 \\ z_2 \end{bmatrix} = \begin{bmatrix} \dot{x} + y \\ x + \ddot{x} + \dot{y} \end{bmatrix}. \tag{17}$$

The remaining states and inputs are expressed as in equation (18) which is detailed in the last column of Table I:

$$\begin{bmatrix} \xi \\ u \end{bmatrix} = \Phi_4\left(z, \dot{z}, \ddot{z}, \dddot{z}, z^{(4)}\right). \tag{18}$$

where

$$g_1(z,\dot{z},\ddot{z},\dddot{z},z^{(4)}) = \frac{(\dot{z}_2 - \ddot{z}_1)(z_1^{(4)} + \ddot{z}_1 - \dddot{z}_2)}{g\sqrt{(\dot{z}_2 - \ddot{z}_1)^2 + (\dddot{z}_1 + \dot{z}_1 - \ddot{z}_2)^2}},$$

$$g_2(z,\dot{z},\ddot{z},\dddot{z}) = \frac{(\ddot{z}_2 - \dddot{z}_1)(\dddot{z}_1 + \dot{z}_1 - \ddot{z}_2)}{g\sqrt{(\dot{z}_2 - \ddot{z}_1)^2 + (\dddot{z}_1 + \dot{z}_1 - \ddot{z}_2)^2}}.$$

Remark 1: These flat outputs are inspired from various sources: the flat output 1 in (11) is the one most employed in the literature while the second flat output in (13) exploits a change of coordinates and the two last flat outputs are derive from the fact that if $[z_1\ z_2]^\top$ is a flat output, then $[z_1\ z_2 + \dot{z}_1]^T$ is also a flat output.

Remark 2: All the flat representations above are found knowing the complete description of the system (inputs, outputs, actuators and the like). There is, however, some works related to "flat input" representation [12]. In this study, proper actuators or inputs are chosen such that a priorly given output becomes a flat output.

B. Trajectory generation using flatness

In equations (4) and (5) we provided a generic motion planning problem and in Section III-A we provided several flat representations. In what follows, we show how the construction of both constraints and costs change depending on the particular flat representation employed.

More specifically, we propose the constraints w_k concerning the position of the UAV which associate with the same amount of time-stamps t_k:

$$\mathbb{W} = \{w_1, w_2, ..., w_N\}, \quad \mathbb{T}_W = \{t_0, t_1, ..., t_N\}. \tag{19}$$

In other words, at the time instant $t_k \in \mathbb{T}_W$, the vector $[x(t_k)\ y(t_k)]^\top$ must satisfy:

$$\begin{bmatrix} x(t_k) \\ y(t_k) \end{bmatrix} = w_k \in \mathbb{W}. \tag{20}$$

Furthermore, the general optimization mentioned in (6) will be replaced by the integral:

$$\mathbf{P} = \arg\min_{\mathbf{P}} \int_{t_0}^{t_N} \left(\dot{x}^2 + \dot{y}^2\right) dt \tag{21}$$

Initially, the constraints (20) and the cost (21) have been given in the position components (x, y) and now, for each flat representation, we rewrite them in terms of the flat output.

1) Cost function with flat output 1: With the representation of flat output 1, we can rewrite the problem (6) with the energy function as:

$$\tilde{\Xi}_1(\mathbf{B}_d(t), \mathbf{P}) = \dot{z}_1^2 + \dot{z}_2^2 = \dot{z}^\top \dot{z}. \tag{22}$$

Similarly, the constraints in (20) are rewritten as:

$$\begin{bmatrix} x(t_k) \\ y(t_k) \end{bmatrix} = \begin{bmatrix} z_1(t_k) \\ z_2(t_k) \end{bmatrix} = w_k. \tag{23}$$

2) Cost function with flat output 2: Similarly, the cost function (21) can be written with the second flat output as:

$$\tilde{\Xi}_2(\mathbf{B}_d(t), \mathbf{P}) = \dot{z}_1^2 + z_1^2 \dot{z}_2^2. \tag{24}$$

The corresponding form of (20) with the flat output (13) is characterized by:

$$\begin{bmatrix} x(t_k) \\ y(t_k) \end{bmatrix} = \begin{bmatrix} z_1(t_k)\cos z_2(t_k) \\ z_1(t_k)\sin z_2(t_k) \end{bmatrix} = w_k. \tag{25}$$

However, it is trivial to show that equation (25) does not give unique solution for $[z_1(t_k)\ z_2(t_k)]^\top$ due to the periodicity of the trigonometric functions. Hence, another way to specify the desired value for the flat output is introduced as:

$$\begin{cases} \begin{bmatrix} x(t_k) \\ y(t_k) \end{bmatrix} = w_k, \\ z_1(t_k) = \sqrt{x(t_k)^2 + y(t_k)^2}, \\ z_2(t_k) = \arctan\dfrac{y(t_k)}{x(t_k)} + 2k\pi. \end{cases} \tag{26}$$

where k can be chosen so that the continuity of $z_2(t)$ will not break the desired direction of the trajectory.

3) Cost function with flat output 3: With the representation of the flat output 3 in (15), we rewrite the problem (21) as:

$$\tilde{\Xi}_3(\mathbf{B}_d(t), \mathbf{P}) = \dot{z}_1^2 + (\dot{z}_2 - \ddot{z}_1)^2. \tag{27}$$

Similarly, the constraints in (20) are indicated as:

$$\begin{bmatrix} x(t_k) \\ y(t_k) \end{bmatrix} = \begin{bmatrix} z_1(t_k) \\ z_2(t_k) - \dot{z}_1(t_k) \end{bmatrix} = w_k. \tag{28}$$

4) Cost function with flat output 4: Equivalently, with flat output 4, we can rewrite the problem (21) as:

$$\tilde{\Xi}_4(\mathbf{B}_d(t), \mathbf{P}) = (\dddot{z}_1 + \dot{z}_1 - \ddot{z}_2)^2 + (\dot{z}_2 - \ddot{z}_1)^2. \tag{29}$$

Similarly, the constraints in (20) are indicated as:

$$\begin{bmatrix} x(t_k) \\ y(t_k) \end{bmatrix} = \begin{bmatrix} z_2(t_k) - \dot{z}_1(t_k) \\ z_1(t_k) + \ddot{z}_1(t_k) - \dot{z}_2(t_k) \end{bmatrix} = w_k. \tag{30}$$

C. Tracking control with feedback linearization

Let us recall the process mentioned in Section II-C, we consider the new input of the system as:

$$u = \begin{bmatrix} u_1 \\ u_2 \end{bmatrix} = \begin{bmatrix} \dot{V}_a \\ \tan\phi \end{bmatrix} = u(z, \dot{z}, \ddot{z}). \tag{31}$$

Then, the virtual input is chosen as:

$$v = \ddot{z}. \tag{32}$$

With such transformation, virtual input (32) will be computed with respect to the linear error dynamics:

$$v = \ddot{z}_{ref} + K_1\dot{e}_z + K_2 \int e_z dt + K_3 e_z, \tag{33}$$

with $e_z = z_{ref}(t) - z(t)$ where $z_{ref}(t)$ is the reference signal and $z(t)$ is the feedback flat output.

However, with the flat representations from (16) and (18), there will exist the derivative of the flat output with the order greater than 2 in the representation of $\dot{V}_a$ and $\tan\phi$. Hence, those two flat output do not meet the condition in (31).

Therefore, using only the representation in (12) and (14), we have the new input:

- for flat output 1 given in (12) :

$$\begin{aligned} \dot{V}_a &= \frac{\ddot{z}_1\dot{z}_1 + \ddot{z}_2\dot{z}_2}{\sqrt{\dot{z}_1^2 + \dot{z}_2^2}}, \\ \tan\phi &= \frac{\ddot{z}_2\dot{z}_1 - \ddot{z}_1\dot{z}_2}{g\sqrt{\dot{z}_1^2 + \dot{z}_2^2}}. \end{aligned} \tag{34}$$

- for flat output 2 given in (14):

$$\begin{aligned} \dot{V}_a &= \frac{\ddot{z}_2\dot{z}_2 z_1^2 + \ddot{z}_1\dot{z}_1 + \dot{z}_2^2\dot{z}_1 z_1}{\sqrt{\dot{z}_1^2 + z_1^2\dot{z}_2^2}}, \\ \tan\phi &= \frac{\ddot{z}_2\dot{z}_1 z_1 - \ddot{z}_1\dot{z}_2 z_1 + 2\dot{z}_1^2\dot{z}_2 + \dot{z}_2^3 z_1^2}{g\sqrt{\dot{z}_1^2 + z_1^2\dot{z}_2^2}}. \end{aligned} \tag{35}$$

Hence, the virtual input v can be formulated as in (36) and computed with the linear dynamics proposed in (33).

$$v = \begin{bmatrix} v_1 \\ v_2 \end{bmatrix} = \ddot{z} = \begin{bmatrix} \ddot{z}_1 \\ \ddot{z}_2, \end{bmatrix} \tag{36}$$

Ultimately, with the flat output (11) and (13), we obtain the two different control laws (37) and (38), respectively:

$$\begin{cases} \dot{V}_a &= \dfrac{v_1\dot{z}_1 + v_2\dot{z}_2}{\sqrt{\dot{z}_1^2 + \dot{z}_2^2}}, \\ \tan\phi &= \dfrac{v_2\dot{z}_1 - v_1\dot{z}_2}{g\sqrt{\dot{z}_1^2 + \dot{z}_2^2}}, \end{cases} \tag{37}$$

$$\begin{cases} \dot{V}_a &= \dfrac{v_2\dot{z}_2 z_1^2 + v_1\dot{z}_1 + \dot{z}_2^2\dot{z}_1 z_1}{\sqrt{\dot{z}_1^2 + z_1^2\dot{z}_2^2}}, \\ \tan\phi &= \dfrac{v_2\dot{z}_1 z_1 - v_1\dot{z}_2 z_1 + 2\dot{z}_1^2\dot{z}_2 + \dot{z}_2^3 z_1^2}{g\sqrt{\dot{z}_1^2 + z_1^2\dot{z}_2^2}}, \end{cases} \tag{38}$$

where v_1 and v_2 are computed from feedback as in (33).

IV. Simulation Result

A. Trajectory generation

For illustration, we use the list of 6 way-points and associated time-stamps taken equidistantly between t_0 and $t_N = 45s$ for the trajectory generation problem:

$$\begin{aligned} \mathbb{W} = 10^2 \times \Bigg\{ &\begin{bmatrix} -1.5 \\ 0.1 \end{bmatrix}, \begin{bmatrix} -1.3 \\ 1 \end{bmatrix}, \begin{bmatrix} -0.1 \\ 1.2 \end{bmatrix}, \\ &\begin{bmatrix} 0.8 \\ 0.1 \end{bmatrix}, \begin{bmatrix} 1.6 \\ -0.9 \end{bmatrix}, \begin{bmatrix} 0.2 \\ -1.2 \end{bmatrix} \Bigg\} \\ \mathbb{T}_W = \{0, 9, 18, 27, 36, 45\}. \end{aligned} \tag{39}$$

Next, we require that all generated states and inputs are continuous. Since the flat output is a weighted sum of spline functions, this means in fact that we have to choose the splines to be of sufficient degree, as detailed in Table II.

Note that each further increase in continuity (e.g., velocity or acceleration are continuous themselves) translates into an incrementation of the B-spline functions' degree.

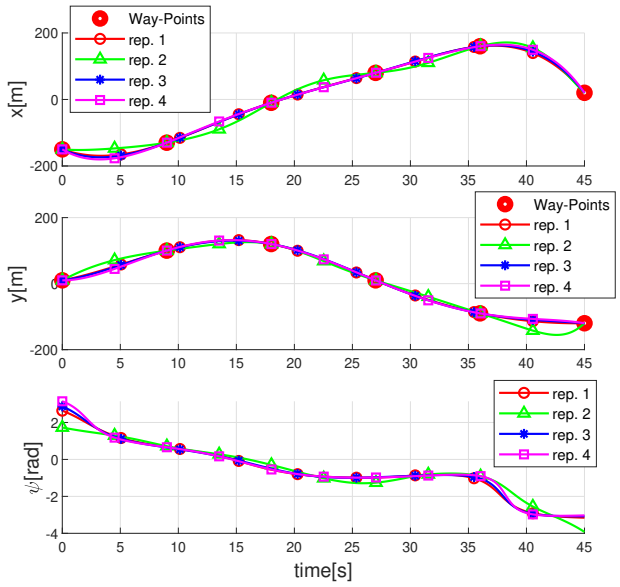

Fig. 1. $x(t)$, $y(t)$ and $\psi(t)$ with 4 flat outputs

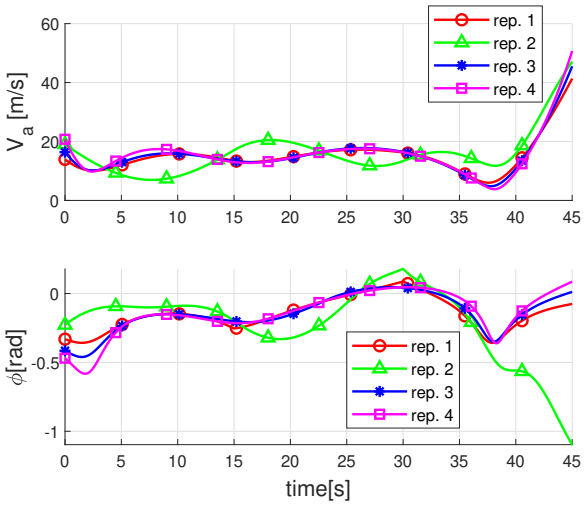

Fig. 2. Input $V_a(t)$ and $\phi(t)$ with 4 flat outputs

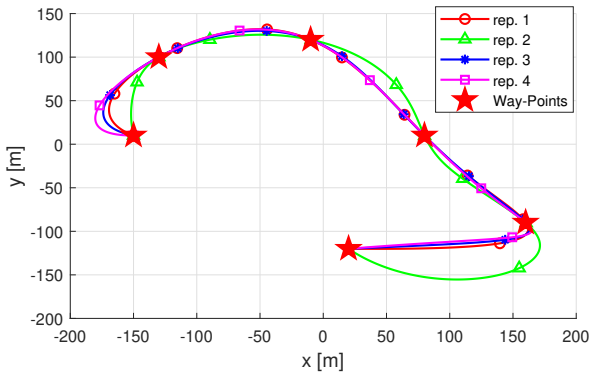

Fig. 3. Position planning with 4 flat outputs

TABLE II
DATA SPECIFICATION AND COMPUTATION RESULTS

	rep. 1	rep. 2	rep. 3	rep. 4
Number of control points	6	6	6	6
Polynomial order of B-spline	3	3	4	5
Cost's value $(\times 10^4 m^2/s)$	1.1332	1.3540	1.1772	1.2580
Curve's length (m)	670.75	709.09	675.46	689.46

Fig. 1 depicts the profiles of the state $\xi(t)$ which are generated with 4 proposed flat representations (12), (14), (16) and (18) respectively. Hereinafter, for simplicity, the 4 aforementioned representations with their corresponding trajectories will be labeled representation as r (rep. r) with $r \in \{1, 2, 3, 4\}$. Similarly, the reference for the inputs is shown in Fig. 2 and the corresponding position is in Fig. 3.

All the reference signals are computed such that they satisfy the optimization problem (21), the constraints in (39) and the continuity constraints, as given in Table II.

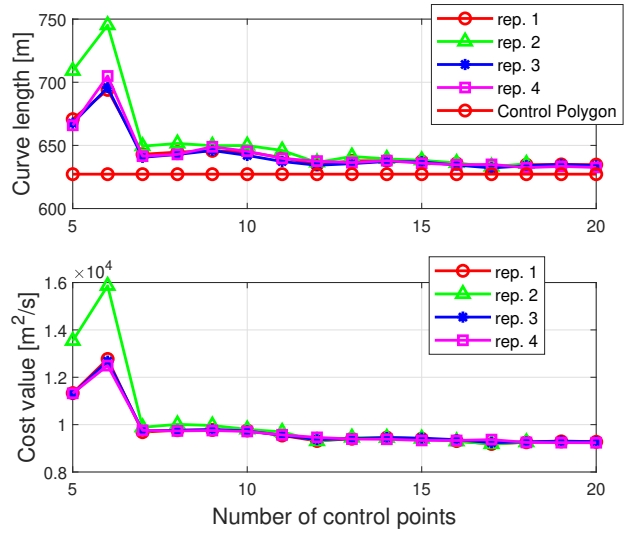

Fig. 4. The the curves' length and objective function values in terms of the number of control points

B. Feedback linearization control

On the other hand, in the control simulation process, we reuse the model (1) and verify it with wind perturbation.

The reference signal is the profile generated with flat output 1 (the curve denoted as rep. 1 in Fig. 3) and simulation data specification is detailed in Table III where the parameters K_1, K_2 and K_3 are chosen from the characteristic equation and its poles p_1, p_2 and p_3 such that:

$$(s - p_1)(s - p_2)(s - p_3) = s^3 - K_3 s^2 + K_1 s + K_2. \quad (40)$$

For the sake of illustration, the poles are chosen identically as $p_1 = p_2 = p_3 = -2$.

TABLE III
SIMULATION SPECIFICATIONS

Control parameters	$K_1 = 12$ $K_2 = 8$ $K_3 = 6$
Wind [m/s]	$W = [W_x, W_y] = [5, 5]$
Simulation time [s]	45s
Sample time [s]	0.01s

In this simulation, the tracking errors will be labeled correspondingly with the control laws proposed in the transformation (34) and (35) as control law 1 (ctrl. law 1) and control law 2 (ctrl. law 2). Details for the errors are given in Fig. 5 for the position x, y and the heading angle ψ.

Besides, in this simulation, we provide 4 different scenarios of wind perturbation vector (W) to experiment on the dependence of the tracking error on the wind direction. Details are provided in Table IV where $RMS(e_{ij})$ is the root mean square value of the tracking error in the i axis $(i \in \{x, y\})$ implemented with the control law j $(j \in \{1, 2\})$.

TABLE IV
TRACKING ERROR WITH DIFFERENT WIND SCENARIOS

RMS(·)[m] / W[m/s]	e_{x1}	e_{x2}	e_{y1}	e_{y2}
[+5;+5]	0.0869	0.1317	0.0588	0.0744
[–5;+5]	0.0675	0.1301	0.1079	0.1146
[+5;–5]	2×10^{21}	1×10^{20}	8×10^{20}	3×10^{20}
[–5;–5]	5×10^{18}	0.3008	3×10^{18}	0.1947

C. Discussions

Let us provide some discussions and insights related to the UAV trajectory generation and tracking when considering various flat representations.

Trajectory generation.

- As expected, from Table II, all the representations can be used to satisfy the way-points constraints. It is also notable that the number of control points needed is not affected by the variation of flat outputs, confirming the unique dependence of the control points on the number of way-points.
- From the parameterization point of view, it can also be seen in the table that the polynomial order of the trajectories are dissimilar, which can be explained with the degree of derivatives existing within each flat output. More specifically, in representation 1 in (12) and 2 in (14), the highest derivative order is 2 while that of representation

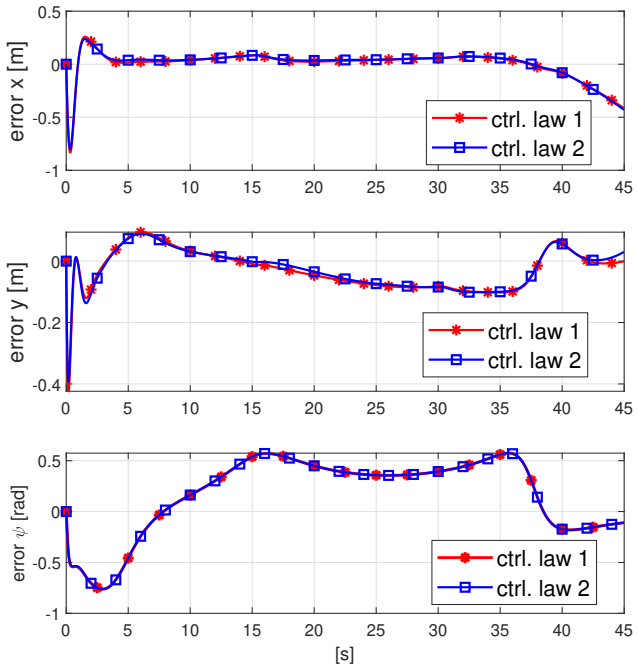

Fig. 5. Tracking error of $x(t)$ and $y(t)$

3 (16) and 4 (18) are 3 and 4, respectively, resulting in different requirement on the B-spline functions' degree to satisfy the continuity constraints.

- Moreover, when the number of control points is considered, the variation of flat representations brings about the differences in not only the curves' length but also the value of the cost function (Fig. 4). Nonetheless, these differences fades when this number gets larger. This can be explained by the convergence of the trajectory to the control polygon, suggesting that after a certain number of control points, there is no use in increasing the number.
- Finally, of interest is also that the cost and path length do not greatly depend on which flat representation is chosen. Still, the complexity of the representation plays a role, by making the problem less (or more so) complex. More precisely, if we look at the representation 1, 3 and 4, the two values increase along with the number of derivative involving in the representations. On the other hand, the second flat output proves more complex, since it contains trigonometric functions, whose periodicity affects the optimization procedure.
- In conclusion, since the curves are constrained in space and time, it comes as no surprise that all the trajectories are relatively similar. Yet, depending on the mathematical expressions inside each representation, each trajectory will have a particular representation.

Trajectory tracking: While the trajectories are distinguishable, the tracking problems seem to have similar behaviors:

- As depicted in Fig. 5, there are differences between the error dynamics of the two control system. These dissimilarities come from the variable where the error dynamic is applied. In detail, the first control law implement the linear dynamic in the first states which are $x(t)$ and $y(t)$. Meanwhile, with the second law, the linearity is applied in the flat output which is a combination of the two first states. However, this property may not have a strong enough impact on the tracking error, thus, the results present little meaningful information.
- However, the results given in Table IV suggest the reliance of the system's performance on both the direction of the wind and the control laws. More particularly, the tracking of the UAV shows better results for the first two scenarios ($W = [+5; +5]$ and $W = [-5; +5]m/s$). On the contrary, when $W = [-5; -5]$, only the control law 2 can stabilize the system and when $W = [+5; -5]$ both of the controllers cannot handle the perturbation.

V. Conclusions

This paper presented the trajectory generation and tracking problem for a fixed-wing UAV. We have shown how multiple flat representations affect various elements of the control architecture. Within the former problem, it is notable that changing the flat output leads to significant changes of the cost function and constraint definitions. The control action is also changed in the latter issue, with implications in what regards closed-loop robustness and performance. As future work, it remains to further analyze complexity of the trajectory generation procedure on one hand and disturbance rejection for the tracking mechanism on the other hand.

References

[1] M. Fliess, J. Lévine, P. Martin, and P. Rouchon, "Flatness and defect of non-linear systems: introductory theory and examples," *International journal of control*, vol. 61, no. 6, pp. 1327–1361, 1995.

[2] F. Stoican, I. Prodan, and D. Popescu, "Flat trajectory generation for way-points relaxations and obstacle avoidance," in *2015 23rd Mediterranean Conference on Control and Automation (MED)*. IEEE, 2015, pp. 695–700.

[3] P. Martin, P. Rouchon, and R. M. Murray, "Flat systems, equivalence and trajectory generation," Ph.D. dissertation, Optimization and Control, 2006.

[4] I. Prodan, S. Olaru, F. Fontes, F. Pereira, J. Sousa, C. STOICA MANIU, and S.-I. Niculescu, *Predictive Control for Path-Following. From Trajectory Generation to the Parametrization of the Discrete Tracking Sequences*. Springer, 12 2015, pp. 161–181.

[5] N. T. Nguyen, I. Prodan, and L. Lefèvre, "Stability guarantees for translational thrust-propelled vehicles dynamics through nmpc designs," *IEEE Transactions on Control Systems Technology*, pp. 1–13, 2020.

[6] ——, "Flat trajectory design and tracking with saturation guarantees: a nano-drone application," *International Journal of Control*, pp. 1–14, 2018.

[7] F. Nicolau and W. Respondek, "Flatness of multi-input control-affine systems linearizable via one-fold prolongation," *SIAM Journal on Control and Optimization*, vol. 55, no. 5, pp. 3171–3203, 2017.

[8] M. Bekcheva, H. Mounier, and L. Greco, "Control of differentially flat linear delay systems with constraints," *IFAC-PapersOnLine*, vol. 50, no. 1, pp. 13 348–13 353, 2017.

[9] M. Franke and K. Robenack, "On the computation of flat outputs for nonlinear control systems," in *Control Conference (ECC), 2013 European*. IEEE, 2013, pp. 167–172.

[10] I. Prodan, F. Stoican, and C. Louembet, "Necessary and sufficient lmi conditions for constraints satisfaction within a b-spline framework," in *2019 IEEE 58th Conference on Decision and Control (CDC)*. IEEE, 2019, pp. 8061–8066.

[11] J.-J. E. Slotine, W. Li *et al.*, *Applied nonlinear control*. Prentice hall Englewood Cliffs, NJ, 1991, vol. 199, no. 1.

[12] F. Nicolau, W. Respondek, and J.-P. Barbot, "Constructing flat inputs for two-output systems," in *The 23rd International Symposium on Mathematical Theory of Networks and Systems*, 2018.